



RESEARCH ARTICLE

Preparation and Characterization of ZnO Nanorods and Analysis of the Effect of Photo Irradiation on the Physical Properties of Polymer Nano Composites

Ahmed Mishaal Mohammed^{1*}, Hameed K. AL-Duliami ² and Marwa A. Mekhlif ¹

¹Department of Chemistry, College of Science, University of Anbar, Ramadi, Iraq.

²Department of Chemistry, College of Education for Pure Sciences, University of Anbar, Ramadi, Iraq.

Received: 23 June 2018

Revised: 25 July 2018

Accepted: 27 Aug 2018

*Address for Correspondence

Ahmed Mishaal Mohammed

Department of Chemistry,
College of Science,
University of Anbar,
Ramadi, Iraq.



This is an Open Access Journal / article distributed under the terms of the **Creative Commons Attribution License** (CC BY-NC-ND 3.0) which permits unrestricted use, distribution, and reproduction in any medium, provided the original work is properly cited. All rights reserved.

ABSTRACT

This study investigated the photodegradation of polyvinyl alcohol (PVA) based nanocomposites with different weight ratios of Zinc oxide (ZnO) nanorods prepared hydrothermally. Scanning electron microscopy, atomic force microscopy, and X-ray diffraction analysis are utilized to study the morphological characteristics and size of ZnO nanorods were studied via, where, films were made by mixing with a polymer solution at different weight percentages of 1%, 2%, 3%, 4%, and 5% and a thickness of $70 \pm 5 \mu\text{m}$. The as-prepared samples were exposed to photoradiation at a wavelength of 356 nm at different time points. The photodegradation of the prepared films with and without additives were assessed with Fourier transform infrared spectroscopy and ultraviolet-visible spectroscopy to monitor the changes in hydroxyl coefficient, carbonyl coefficient and dissociation constant (K_d), which was used to illustrate the effect of ZnO nanorod addition. The prepared ZnO nanorods showed a wide range of applications in PVA photodegradation. In addition to the mean chain scission and degradation degree, the molecular weight and chain scission decreased in the presence of the ZnO nanorods, and this observation was consistent with that described in other studies.

Keywords: Zinc oxide, Polymer, Photodegradation, Polyvinyl alcohol.

INTRODUCTION

Nanotechnology involves the preparation of nanoscale materials [1]. ZnO is one of the versatile and technologically important semiconducting materials that exhibit a direct and wide band gap (3.3eV). It has been extensively explored because of its electrical, and piezoelectric [2-6], chemical [7], optical [8], and magnetic [9] properties. ZnO has also



**Ahmed Mishaal Mohammed et al.**

been recognized as an important material because of its wide applications, such as catalysts [10], semiconductors [11], gas sensors [12], ultraviolet (UV)-shielding materials [13], piezoelectric devices [14], photochemicals [15], polymer coatings [16], and antibacterial agents [17]. ZnO is a multifunctional material, as such, studies on ZnO nanoparticles have focused on their preparation through various methods, including solid-state reaction [9], microwave-assisted method [18], flame spray pyrolysis [19], sol-gel method [20], hydrothermal method [21], sonochemical route [22], and mechanochemical methods [23]. ZnO films have been prepared via several techniques, such as electrochemical deposition [24], chemical vapor deposition (CVD) [25], hydrothermal or solvothermal methods [26], spray pyrolysis technique [27], electrodeposition [28], chemical bath deposition [29], sputtering [30], metal-organic CVD [31], evaporation [32], molecular beam epitaxy, atomic layer epitaxy [33, 34], and pulsed laser deposition [35]. According to the importance of polyvinyl alcohol (PVA) as water-soluble transparent polymer extensively, it has been used in industries, as well as, it is considered as an excellent physical and chemical properties, good chemical resistance, non-toxicity, biodegradability, good film formation capacity, and high crystal modulus. The fact is that, PVA is utilized in as hydrolyze form with 85% hydrolysis degree [36]. Indeed, it is a polymer which has various pharmaceutical, biomedical, and technological applications [37]. For example, it can be applied to coat ZnO [38], Ag [39], and titanium dioxide [40]. In this study, a new type of ZnO nanorods was prepared by using hydrothermal method and used as a UV photoinducer for PVA degradation.

MATERIALS AND METHODS

Chemicals

It is important to note that the deionized distilled water was involved to make all the solutions. In addition, the standard metal ion solution, Zinc nitrate hexahydrate [$\text{Zn}(\text{NO}_3)_2 \cdot 6\text{H}_2\text{O}$], was commercially obtained from Aldrich. Anyhow, the analytical grade of this study was based on all of the chemicals and reagents.

Growth Layer Preparation

In this process, 0.5 g of zinc nitrate, 5 g of hexamethylenetetramine, and 100 ml of deionized water were placed in a beaker and mixed using a magnetic stirrer for 1 hrs. At room temperature. The prepared growth layer solution was placed in another beaker where seed-coated substrates were immersed. The resulting mixture was kept in an oven at 90°C for 3 hrs. Slides were taken out from the beaker and rinsed with water to separate residuals. The substrates were subjected to annealing at 500°C for 1 hrs. The ZnO nanorods were prepared at pH values of 7.5.

Sample

The first step of preparing the specimens which represented by films was based on dissolving PVA with a constant concentration of 10% w/v of the polymer solution, where, this polymer dissolved in deionized water at 40 °C. This stock solution was mixed with 1ml of the used ZnO nanorods as the stabilizer of weight ratios (1% , 2% , 3% , 4% , and 5%) and casted using glass flakes to form PVA films with a thickness of $70 \pm 5 \mu\text{m}$. The films were then cut into parts of 1.5 cm x 3 cm for measurements.

The Samples Irradiation

An accelerated irradiator, assembled to the one in a laboratory, supplied with a power of 125 Watts and a light filter with a length of 356 nm for 16 hrs. was used to irradiate the specimens. Under many circumstances, the samples were located in vertical and parallel orientations subjected to the lamp to make sure that the light fell on vertically over the films tube. Therefore, the films positions periodically were changed to ensure the light coincidence. Polymeric films with and without PVA were irradiated with UV at different periods, ranging from 4 hrs. to 16 hrs. (Table 2).



**Ahmed Mishaal Mohammed et al.**

The Studies of Spectral

Variations of the polymeric films were examined through fouriertransformer infrared (FT-IR) spectroscopy, measurementof the growth level of the hydroxyl group (I_{OH}) and carbonyl group (I_{CO}) as means of PVA degradation behavior under light of fact, and UV measurements to determine the absorbed band intensities calculated before and after irradiation was administered [41].

Morphological analysis

Morphological analysis is mainly performed to describe the state of degradation. In this process, molecules become reflected on a polymer surface because of the effect of high-energy light (UV), thereby changing the color of the surface or the color of the whole polymer this phenomenon reflects the loss of the physical, andelectrical,mechanical properties, thereby causing softness and pitting on external surfaces [42].

Material Characterization

X-ray diffraction (XRD) with $CuK\alpha$ radiation ($\lambda = 1.5418 \text{ \AA}$) was conducted to investigate the phase composition and crystalline properties of the sample.The quality of surface morphology and the quantity of elemental composition were analyzed through scanning electron microscopy (SEM) and atomic force microscopy (AFM).The chemical functional groups of the sample that did not undergo annealing were characterized through FT-IR.

RESULTS AND DISCUSSION

Structural Characterization

Fig. 1 shows the XRD pattern of the sample powder compared with that of ICDD no 01-076-0704 as the standard reference of the ZnO phase. The diffraction peaks indexed to (100), (002), (101), (102), (110), (103), and (112) planes were observed, confirming the ZnO hexagonal wurtzite structure. The scanned 2θ axis of the XRD graph, showed that three strong peaks at 31.73° , 34.38° , and 36.20° were attributed to (100), (002), and (101) ZnO planes, respectively (Table 1).

SEM Measurements

We identified the morphological characteristic and structures of the particles and measured the grain size of the samples prepared hydrothermally.Fig.2shows the SEM micrograph of the ZnO nanorodssynthesized hydrothermally at different magnifications.

AFM Measurements

AFM is essential for studying the morphological characteristics of ZnO nanorods. Quantitative information from individual ZnO can be generated through the software-based image processing of AFM data. Individual particles determination was based on the size information (length, width, and height) and other physical properties (morphological characteristics and surface texture).AFM can be functioned in liquid or gas media, therefore, this capability is considered as highly advantageous for the characterization of ZnO. In our study, AFM was applied to analyze the morphological characteristics and size of the particles and the topography of the ZnO surface structure. As noticed in Fig. 3, the AFM images presenting the two - and three-dimensional views of the surface structure of the ZnO nanorods, which were grown hydrothermally. The images indicated that the ZnO nanorods had small particles size distribution with a diameter of 52.16 nm



**Ahmed Mishaal Mohammed et al.**

FT-IR Spectroscopy

The FT-IR spectra of all of the samples, palletized with KBr were recorded from 400 cm^{-1} to 4000 cm^{-1} (Fig. 5). The spectra consisted of seven vibrational bands. The transmittance spectrum of the as-deposited ZnO film showed the main absorption bands centered at 1222.79 and 3431.13 cm^{-1} , and several small features were located at 528.46, 867.91, 1504.37, 1635.52, 2329.85, 2887.24 and 3014.53 cm^{-1} . The absorption bands that centered at 484.10 and 528.46 cm^{-1} could be associated with ZnO bond vibration, compared with that of the standard FT-IR of the ZnO powder. A strong peak at 3431.13 cm^{-1} was observed in the as-deposited ZnO film, which is sensitive to the stretching vibrations of –OH [28]. The other absorption bands at 2887.24, 1635.52, and 867.91 cm^{-1} can be related to N–H and, N–O bonds [30].

UV–vis Spectroscopy

The process of characterizing the optical absorption properties of the ZnO nanorods involved conducting UV–vis spectroscopy, where, the UV–vis absorption spectra of the samples was achieved at a room temperature [43] and were recorded in the wavelength range of 200–800 nm through a Shimadzu UV 3600 UV–vis–NIR spectrometer (Shimadzu Corporation, Kyoto, Japan). The photodegradation of the PVA films at different concentrations was studied through UV–vis spectroscopy, by exposing the PVA films to UV radiation for a given period to change the color of the films to yellowish. This change indicated the photolysis of the polymer (Table 2). Through observing the absorption spectrum in terms of time irradiation, these films varied and reflected when calculating the rate of decomposition (K_d) via recording the absorption spectrum of UV and during the process at different times of irradiation. We observed that the absorption spectrum of these films varied in terms of the time of irradiation as shown in Fig. 6.

The rate of change in the absorption spectrum with respect to the time of irradiation was dependent on the ZnO nanorod additive concentration, which increased as the ZnO nanorod concentration increased due to the increase in the active substance content (Figs. 7–11). To calculate the rate constant of the photolysis of polymeric films in the presence of the ZnO nanorod additive, where, the relationship between the time of irradiation and the logarithm of absorption ($A_\infty - A_t$) was drawn as shown in (Figs. 12–16). The slope apparently shown as a straight line, indicating that the interaction light of this ZnO nanorod was of the first class, which was the constant determinant rate of photolysis (K_d) at various concentrations under the same conditions was previously determined as noticed in (Table 3). This result suggested that K_d was sensitive to additive concentrations, whose increase was consistent with those described in previous studies [44]. This finding confirmed that the additive accelerated the interaction between the light and polymer.

FT-IR Spectrum of PVA

The exposure of pure PVA to high-energy rays with a wavelength of 356 nm altered the FT-IR spectrum [45] and yielded two broad bands. The first band of the carbonyl group (C=O) appeared at 1600–1700 cm^{-1} , which increased with irradiation time [46]. This band was present with few values before the films were irradiated because of the stress induced by thermal oxidation during manufacturing (Fig. 17). The second band of the hydroxyl and hydroperoxide polymer appeared at 3200–3600 cm^{-1} , where the absorbance increased as the ZnO concentration increased (Fig. 19). Therefore, the coefficients of the increase in the absorption of I_{OH} and I_{CO} were high at high additive concentrations (Tables 4, and 5 and Figs. 20 and 21) as calculated using the base-line method [47]. These results showed correspondence of the values calculated from the decomposition constant values (highest K_d). The calculations via the viscometer method showed the average molecular weight of the polymeric film before and after addition, suggesting that the average molecular weight decreased as the irradiation time was extended. The additive concentration of the ZnO nanorod was comparable with that of the reference because of the fragmentation of the polymeric chains (Tables 6, and 7), and the viscous molecular weight rapidly decreased at the beginning of





Ahmed Mishaal Mohammed et al.

irradiation [48]. Consequently, the most apparent results revealed that the bonds between the polymer chains were formed randomly along the polymeric chain, where, this observation was firmly established by the linear relationship of the average chain scission (S) and the degree of degradation (α) through time [44], revealing that S and α of the chips of pure PVA were less than those supported by the ZnO nanorod additive. This study provided a basis for using ZnO nanorods as a good catalyst to photodegrade plastic materials, reduce environmental pollution, and accelerate their decomposition.

CONCLUSION

Rod-like ZnO nanorods were successfully synthesized hydrothermally in a nanosize range with a diameter of approximately 52.16 nm. The synthesized ZnO nanopowder obtained exhibited good crystallinity. The addition of ZnO nanorods increased the photodegradation rate because of the absorption of UV light. The degradation rate increased when the nanorods were exposed to irradiation for 16 hrs. By studying the impact of different concentrations of ZnO nanorods on polymer degradation, we found that the rate of polymer degradation increased as the concentration of each ZnO nanorod increased. These results and the calculated average viscous molecular weight, average numerical S , and α confirmed the increase in the photodegradation rate.

REFERENCES

1. Zhou, B. and Balee, R., "Groenendaal, nanoparticle and nanostructure catalysts: technologies and markets", *Nanotech. Law Business*, Vol. 2, 222-231(2005).
2. Tang, Z. K., Wang, G. K., Yu, P., Kawasaki, M., Ohtomo, A., Koinuma, H. and Segawa, Y., "Room-temperature ultraviolet laser emission from self-assembled ZnO microcrystallite thin films", *Appl. Phys. Lett.* Vol. 72(25), 3270 - 3278(1998).
3. Kind, H., Yan, H., Law, M., Messer, B. and Yang, P., " Nanowire ultraviolet photodetectors and optical switches", *Adv. Mater.* Vol. 14, 158 - 164(2002).
4. Suchada, W., Tomoaki, M., Yoshinori, H., Yoichiro, N., Hidenori, M., and Wisanu, P., "Synthesis and characterization of ZnO nanorods by hydrothermal method ", *Materialstudy: Proceedings*, Vol. 5 (5) , 10964 - 10969 (2018).
5. Pushpitha, R., Bruno, L., Sahuban, M., Chandramohan, R., and Srikumar, S., "Preparation and characterization of Mn doped ZnO nanorods" , *Physics of the Solid State*, Vol. 60 (5), 1011 - 1015 (2018).
6. Youngjo, T., Dongseok, P., and Kijung, Y., "Characterization of ZnO nanorod arrays fabricated on Si wafers using a low-temperature synthesis method", *Journal of Vacuum Science & Technology B*, Vol. 24, 2047 - 2052 (2006).
7. Suwanboon, S., Amornpitoksuk, P., Bangrak, P. and Randorn, C., "Physical and chemical properties of multifunctional ZnO nanostructures prepared by precipitation and hydrothermal methods", *Ceramics International*, Vol. 40, 975- 983(2014).
8. Labuayai, S., Promarak, V. and Maensiri, S., "Synthesis and optical properties of nanocrystalline ZnO powders prepared by a direct thermal decomposition route", *Applied Physics A*, Vol. 94, 755 – 761(2009).
9. Yilmaz, S., Nisar, J., Atasoy, Y., McGlynn, E., Ahuja, R., Parlak, M. and Bacaksız, E., "Defect-Induced room temperature ferromagnetism in B-Doped ZnO", *Ceramics International*, Vol. 39, 4609-4617(2013).
10. Suwanboon, S., Amornpitoksuk, P., Sukolrat, A. and Muensit, N., "Optical and photocatalytic properties of La-Doped ZnO nanoparticles prepared via precipitation and mechanical milling method", *Ceramics International*, Vol.39, 2811-2819(2013).
11. Zhang, C., "The influence of post-growth annealing on optical and electrical properties of P-Type ZnO films", *Materials Science in Semiconductor Processing*, Vol. 10, 215-221(2007).
12. Yu, A., Qian, J., Pan, H., Cui, Y., Xu, M., Tu, L., Chai, Q. and Zhou, X., "Micro-Lotus constructed by Fe-Doped ZnO hierarchically porous nanosheets: preparation, characterization and gas sensing property", *Sensors and Actuators B: Chemical*, Vol. 158, 9-16(2011).



**Ahmed Mishaal Mohammed et al.**

13. Li, R., Yabe, S., Yamashita, M., Momose, S., Yoshida, S., Yin, S. and Sato, T. , "Synthesis and UV-shielding properties of ZnO- and CaO-Doped CeO₂ via soft solution chemical process", *Solid State Ionics*, Vol. 151, 235-241. (2011).
14. Seo, M., Jung, Y., Lim, D., Cho, D. and Jeong, Y., "Piezoelectric and field emitted properties of controlled ZnO nanorods on CNT yarns", *Materials Letters*, Vol. 92, 177-180(2013).
15. Mousa, M., Bayoumy, W. and Khairy, M., "Characterization and photo-chemical applications of Nano-ZnO prepared by wet chemical and thermal decomposition methods", *Materials Research Bulletin*, Vol. 48, 4576-4582(2013).
16. Qin, L., Shing, C., Sawyer, S. and Dutta, P.S., "Enhanced ultraviolet sensitivity of zinc oxide nanoparticle photoconductors by surface passivation", *Optical Materials*, Vol. 33, 359-362(2011).
17. Talebian, N., Amininezhad, S.M. and Doudi, M. "Controllable synthesis of ZnO nanoparticles and their morphology-dependent antibacterial and optical properties", *Journal of Photochemistry and Photobiology B: Biology*, Vol. 120, 66-73 , (2013).
18. Sharma, D., Sharma, S., Kaith, B., Rajput, J. and Kaur, M., "Synthesis of ZnO nanoparticles using surfactant free in-air and microwave method", *Applied Surface Science*, Vol. 257, 9661-9672(2011).
19. Lee, S.D., Nam, S.H., Kim, M.H. and Boo, J.H., "Synthesis and photocatalytic property of ZnO nanoparticles prepared by spray-pyrolysis method", *Physics Procedia*, Vol. 32, 320-326(2012).
20. Ba-Abbad, M.M., Kadhum, A.A.H., Bakar, M., A., Takriff, M.S. and Sopjan, K. 'The effect of process parameters on the size of ZnO nanoparticles synthesized via the sol-gel technique', *Journal of Alloys and Compounds*, Vol. 550, 63-70(2013).
21. Aneesh, P.M., Vanaja, K.A. and Jayaraj, M.K., "Synthesis of ZnO nanoparticles by hydrothermal method", *Proceedings of SPIE*, Vol. 6639, 66390J-1-66390J-9(2007).
22. Kazeminezhad, I., Sadollahkhani, A. and Farbod, M., "Synthesis of ZnO nanoparticles and flower-like nanostructures using nonsono- and sono-electrooxidation methods", *Materials Letters*, Vol. 92, 29-32(2013).
23. Stanković, A., Veselinović, L., Škapin, S., Marković, S. and Uskoković, D., "Controlled mechanochemically assisted synthesis of ZnO nanopowders in the presence of oxalic acid", *Journal of Materials Science*, Vol. 46, 3716-3724(2011).
24. Elias, J., Tena-Zaera, R, and Levy-Clement, C., "Effect of the chemical nature of the anions on the electrodeposition of ZnO nanowire arrays", , *J. Phys. Chem. C*, Vol. 112 (15) 5736-5741(2008).
25. Sato, H., Minami, T., Miyata, T., Takata, S., Ishii, M., "Transparent conducting ZnO thin films prepared on low temperature substrates by chemical vapour deposition using Zn(C₅H₇O₂)₂", *Thin Solid Films*, Vol. 246 (1-2), 65-70 (1994).
26. Yang, H., Song, Y., Li, L., Ma, J., Chen, D., Mai, S., Zhao, H., "Large-scale growth of highly oriented ZnO nanorod arrays in the Zn-NH₃-H₂O hydrothermal system", *Cryst. Growth Des.*, Vol. 8 (3), 1039-1043 (2008).
27. Ambia, M. G., Islam, M. N., and Hakim, M. O., " The effects of deposition variables on the spray pyrolysis of ZnO thin film", *J. Mater. Sci.* Vol. 29 (24) 6575-6580 (1994).
28. Izaki, M., " Transparent zinc oxide films prepared by electrochemical reaction", *Appl. Phys. Lett.* Vol. 68, 2439-2445 (1996).
29. Ennaoui, A., Weber, M., Scheer, R., Lewerenz, H. J., "Chemical-bath ZnO buffer layer for CuInS₂ thin-film solar cells", *Sol. Energy Mater. Sol. Cells* Vol. 54(1-4), 277-286 (1998).
30. Stolt, L., Hedstrom, J., Ruckh, M., Kessier, J., Velthaus, K. O. and Schock, H. W., "ZnO/CdS/CuInSe₂ thin-film solar cells with improved performance", *Appl. Phys. Lett.* Vol. 62 , 597-604 (1993).
31. Wenas, W., Yamada, A., Konagai, M. and Takahashi, K., "Metalorganic chemical vapor deposition of ZnO using D₂O as oxidant", *J. J. Appl. Phys.* Vol. 33 (3A), 283-290 (1994).
32. Huang, M. H., Wu, Y., Feick, H., Weber, E., Yang, P., " Catalytic growth of zinc oxide nanowires by vapor transport", *Advances Mater.* Vol. 13 , 113-119 (2001).
33. Sang, B., Konagai, M., "Growth of transparent conductive oxide ZnO films by atomic layer deposition", *J. J. Appl. Phys.* Vol. 35 (5B), 602-608 (1996).





Ahmed Mishaal Mohammed et al.

34. Steven, C., and John, L., "Atomic layer epitaxy of aluminum nitride: Unraveling the connection between hydrogen plasma and carbon contamination", *ACS Appl. Mater. Interfaces*, Vol. 10 (23), 20142-20149 (2018)
35. Zhang, Y., Russo, R. E., Mao, S. S., "Femtosecond laser assisted growth of ZnO nanowires", *Appl. Phys. Lett.* Vol. 87, 133115 – 133118 (2005).
36. Wang, H.H., Shyr, T.W. and Hu, M.S., "The elastic property of polyvinyl alcohol gel with boric acid as a cross-linking agent", *Journal of Applied Polymer Science*, Vol.74, 3046-3052(1999).
37. Scotchford, C., Cascone, M., Downes, S. and Giusti, P., "Osteoblast responses to collagen-PVA bioartificial polymers *in Vitro*: The effects of cross-linking method and collagen content", *Biomaterials*, Vol. 19, 1-11(1998).
38. Chandrakala, H., Ramaraj, B. and Lee, J.H., "Polyvinyl alcohol/carbon coated zinc oxide nano-composites: Electrical, optical, structural and morphological characteristics", *Journal of Alloys and Compounds*, Vol. 580, 392-400(2013).
39. Shin, J., Kim, Y., Lee, K., Lim, Y.M. and Nho, Y.C., "Significant effects of sodium acetate, an impurity present in poly(vinyl alcohol) solution on the radiolytic formation of silver nanoparticle" , *Radiation Physics and Chemistry*, Vol. 77, 871-876(2008).
40. Hebeish, A., Abdelhady, M. and Youssef, A., "TiO₂nanowire and TiO₂nanowire doped Ag-PVP nano-composite for antimicrobial and self-cleaning cotton textile" , *Carbohydrate Polymers*, Vol. 91, 549-559(2013).
41. Skuzina, S.I. and Mikhailov, A.I., "Institute of problems of chemical physics russian academy of science, high energychemistry, Vol. 44 (1), 667-673 (2010).
42. Taraq, A., J., "Copolymerization study of (N-Acryloyl Amide) monomer with butyl acrylate and determination of the reactivity ratio", *Journal of Pure Science*, Vol. 1 (2), 80-88 (2007).
43. Cimitan, S., Albonetti, S., Forni, L., Peri, F., Lazzari, D., " Solvothermal synthesis and properties control of doped ZnO nanoparticles", *J. Colloid. Interface Sci.*, Vol. 329, 73-80 (2009).
44. Hameed K., and Abdul Hameed H., "A study of effect of copper (II)-complex (Cu-BHBH) on the photo degradation of poly styrene films", *International Journal of Applied and Natural Sciences*, Vol. 3 (3), 123-134 (2014).
45. Yang, J., Wang, Y., Kong, J., Jia, H., and Wang, H., "Synthesis of ZnO nanosheets via electrodeposition method and their optical properties, growth mechanism" , *Opt. Mater.*, Vol. 46 , 179-185 (2015).
46. Li, X., Cheng, S., Deng, S., Wei, X., Zhu, J., and Chen, Q., "Direct observation of the layer-by-layer growth of ZnO nanopillar by in situ high resolution transmission electron microscopy", *Sci. Rep.*, Vol. 7, 40911-40919 (2017).
47. Belkhalifa, H., Ayed, H., Hafdallah, E., Aida, A., and Ighil, R., "Characterization and studying of ZnO thin films deposited by spray pyrolysis: effect of annealing temperature" , *Optik*, Vol. 127(4) , 2336-2340(2016).
48. Gawali, S., Mahadik, S., Pedraza, F., Bhosale, C., Pathan, H., Jadkar, S., "Synthesis of zinc oxide nanorods from chemical bath deposition at different pH solutions and impact on their surface properties", *J. Alloy. Compd.*, Vol. 704, 788-794(2017).

Table 1. The structural parameters of ZnO nanorods as obtained from XRD analysis.

hk1	2θ(degree)	
	Observed	JCPDS
100	31.73°	31.76°
002	34.38°	34.42°
101	36.20°	36.25°
102	47.54°	47.53°
110	56.56°	56.60°
103	62.80°	62.86°
112	67.80°	67.96°





Ahmed Mishaal Mohammed et al.

Table 2. Absorbance values of the PVA with thickness 70±5 µm containing different concentrations of the ZnO nanorods and calculated at 283.5 nm spectrum measurements of UV-Vis with time

Irradiation Time (hrs.)	Absorbance				
	0.0	4	8	12	16
Concentration %					
PVA	0.108	0.137	0.160	0.200	0.273
PVA + 1 % ZnO	0.111	0.243	0.310	0.412	0.486
PVA + 2 % ZnO	0.112	0.364	0.607	0.685	0.850
PVA + 3 % ZnO	0.113	0.466	0.723	0.802	0.916
PVA + 4 % ZnO	0.114	0.543	0.825	0.932	1.100
PVA + 5 % ZnO	0.117	0.573	0.884	0.994	1.215

Table 3. Values constants of rate decomposition K_d of the ZnO nanorods in PVA films

Concentrations %	$K_d(\text{Sec})^{-1} \times 10^4$
1	5.361
2	6.245
3	6.541
4	6.7417
5	6.789

Table 4. Coefficient growth values carbonyl (I_{CO}) with irradiation time for PVA containing concentrations different of the ZnO nanorods

Irradiation time (hrs.)	Carbonyl Index (I_{CO})				
	0.0	4	8	12	16
Wt. % of Addition					
PVA	0.378	0.551	0.649	0.800	0.902
PVA + 1 ZnO	0.396	0.632	0.683	0.839	1.173
PVA + 2 ZnO	0.401	0.666	0.831	1.008	1.400
PVA + 3 ZnO	0.439	0.965	1.045	1.183	1.608
PVA + 4 ZnO	0.469	0.993	1.293	1.373	1.930
PVA + 5 ZnO	0.496	1.066	1.379	1.632	2.121

Table 5. Coefficient growth values hydroxyl (I_{OH}) with irradiation time for PVA containing concentrations different of the ZnO nanorods

Irradiation time (hrs.)	Carbonyl Index (I_{OH})				
	0.0	4	8	12	16
Wt. % of Addition					
PVA	0.272	0.505	0.563	0.733	0.810
PVA + 1 ZnO	0.282	0.586	0.625	0.793	1.113
PVA + 2 ZnO	0.303	0.655	0.706	0.982	1.252
PVA + 3 ZnO	0.340	0.839	0.954	1.086	1.582
PVA + 4 ZnO	0.393	0.860	1.195	1.287	1.747
PVA + 5 ZnO	0.408	0.933	1.270	1.551	2.069





Ahmed Mishaal Mohammed et al.

Table 6. Values calculated from measuring of the viscous molecular weight for pure PVAchips

Time Irradiation (hrs.)	$(\overline{M}_v) \times 10^3$	$(M_v)^2 \times 10^9$	$\frac{dM_v}{dt} = \frac{M_{v0} - M_{vt}}{t}$	Degree of Polymerization P	$\frac{1}{P} \times 10^{-4}$	Deg. Degree $a \times 10^{-3}$	Ava. Chain Scission (S)
0	51.404	2.642	∞	1168.272	8.559	0.0	0.0
4	41.591	1.729	0.681	945.250	10.579	0.202	0.235
8	35.809	1.282	0.541	813.840	12.278	0.371	0.433
12	31.405	0.986	0.462	713.750	14.010	0.545	0.636
16	28.379	0.805	0.399	644.977	15.504	0.694	0.810

Table 7. Values calculated from measuring of the viscous molecular weight for PVA with concentration 4 %ZnO nanorods

Time Irradiation (hrs.)	$(\overline{M}_v) \times 10^3$	$(M_v)^2 \times 10^9$	$\frac{dM_v}{dt} = \frac{M_{v0} - M_{vt}}{t}$	Degree of Polymerization P	$\frac{1}{P} \times 10^{-4}$	Deg. Degree $a \times 10^{-3}$	Ava. Chain Scission (S)
0	51.404	2.642	∞	1168.272	8.559	0.0	0.0
4	38.282	1.465	0.911	870.045	11.493	0.293	0.342
8	31.988	1.023	0.674	727.000	13.755	0.519	0.606
12	27.925	0.779	0.543	634.659	15.756	0.719	0.839
16	24.603	0.605	0.465	559.159	17.884	0.932	1.088

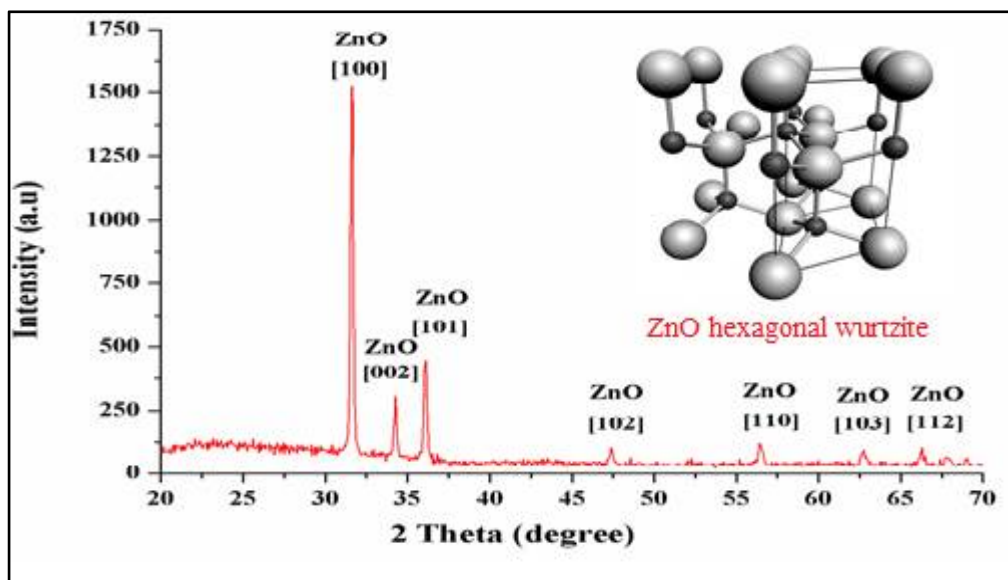


Fig.1. X-ray diffraction pattern of ZnO nanorods compared to standard ZnO phase (ICDD no 01-076-0704).





Ahmed Mishaal Mohammed et al.

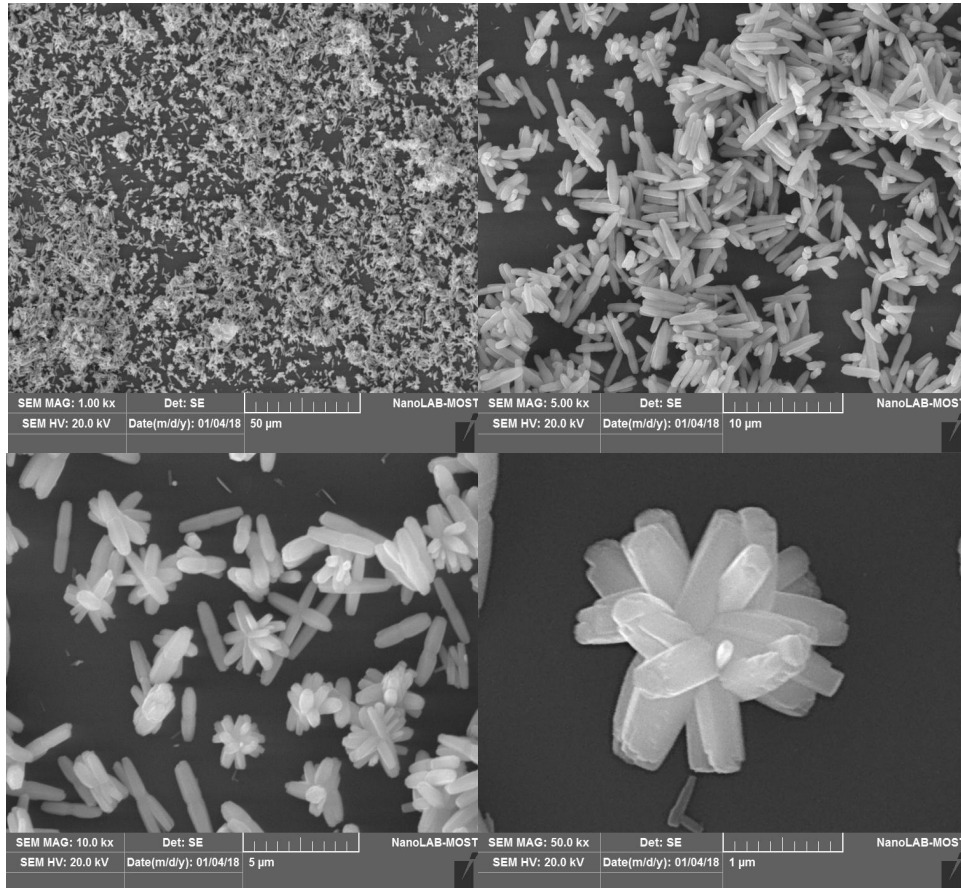


Fig. 2. SEM micrograph of ZnO nanorods synthesized in different magnification

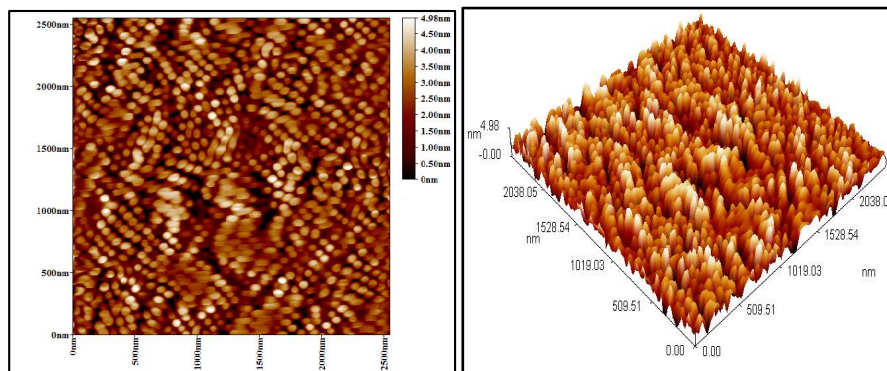


Fig. 3. AFM image of 2-dimensional and 3-dimensional of ZnO nanorods





Ahmed Mishaal Mohammed et al.

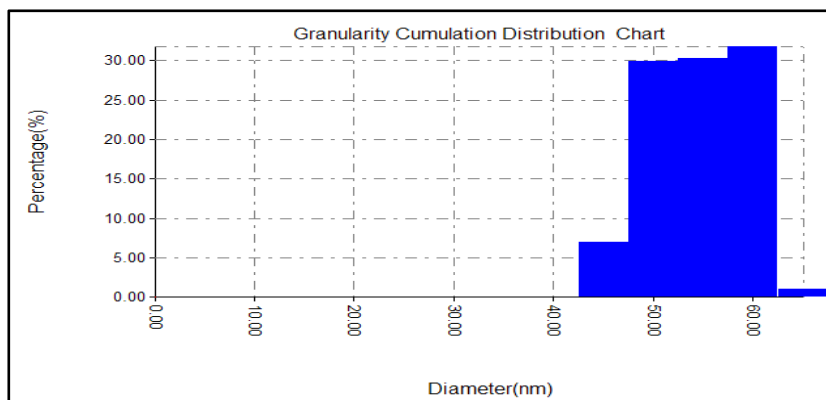


Fig.4. The average distribution for ZnO nanorods of diameter 52.16 nm

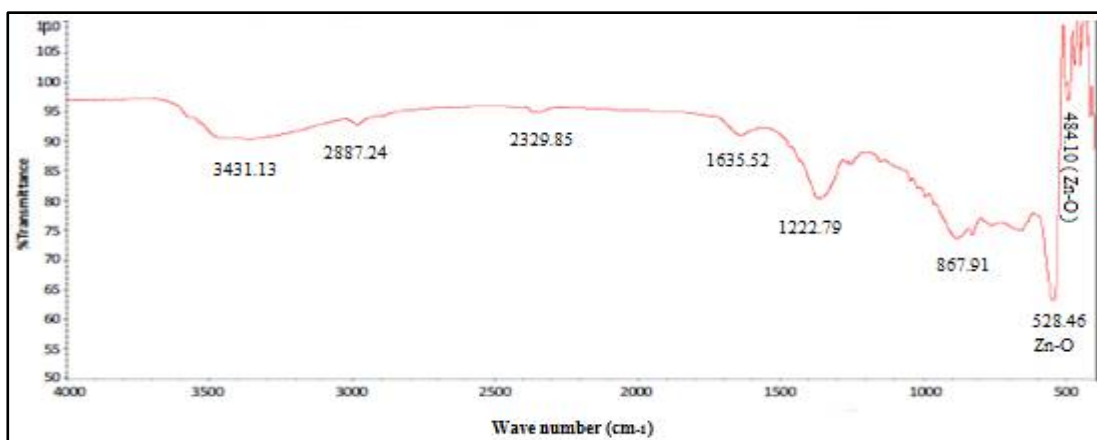


Fig. 5. FT-IR spectrum of ZnO nanorods

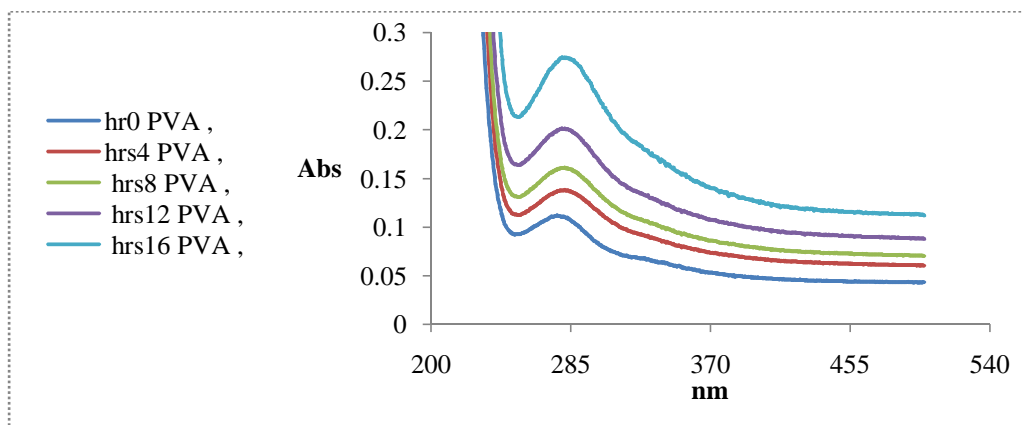


Fig.6. Change in the spectrum of UV-Vis for pure PVA with thickness $70 \pm 5 \mu\text{m}$ at different times of irradiation





Ahmed Mishaal Mohammed et al.

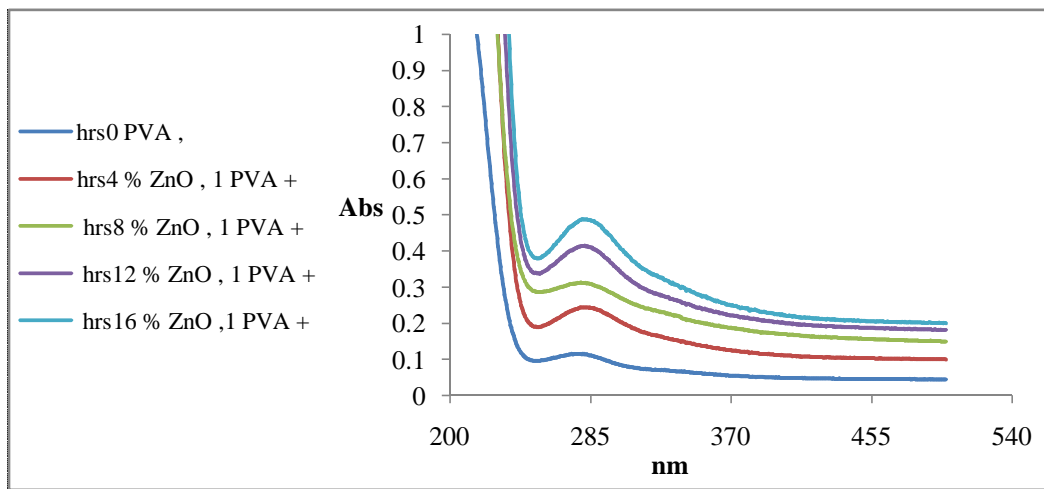


Fig.7.Change in the spectrum of UV–Vis for PVAcontaining concentration (1%) of the ZnO nanorods with thickness $70\pm 5 \mu\text{m}$ at different times of irradiation

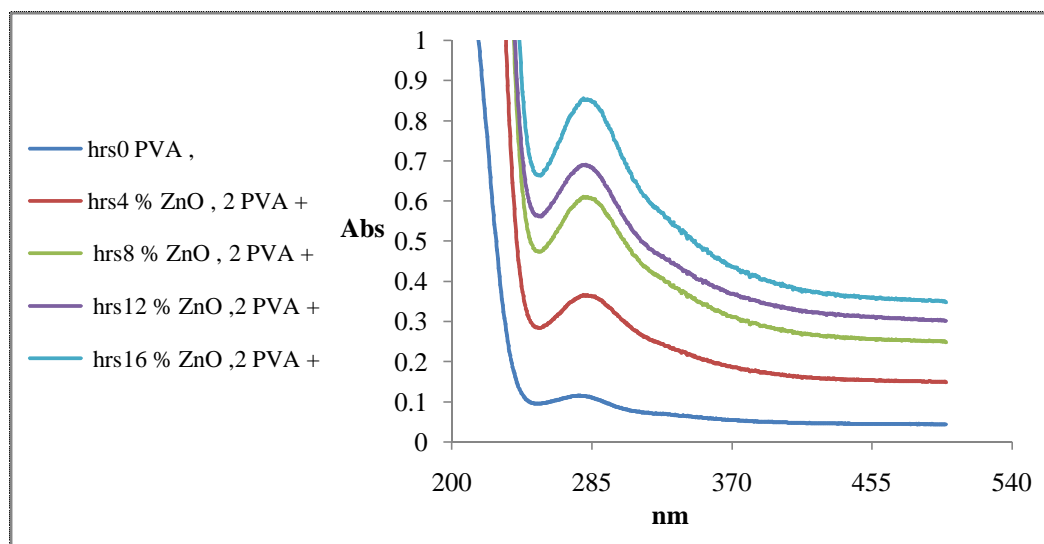


Fig. 8.Change in the spectrum of UV–Vis for PVAcontaining concentration (2%) of the ZnO nanorods with thickness $70\pm 5 \mu\text{m}$ at different times of irradiation





Ahmed Mishaal Mohammed et al.

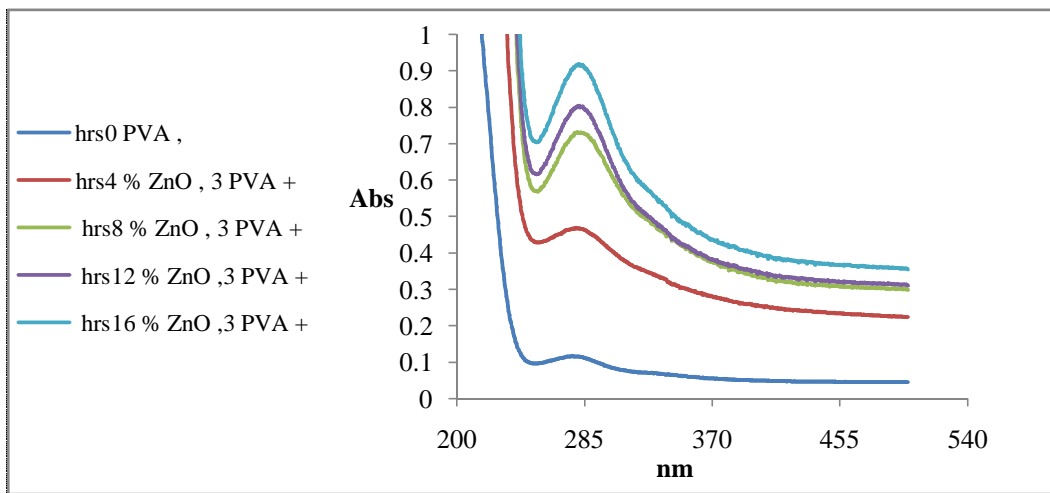


Fig. 9.Change in the spectrum of UV–Vis for PVAcontaining concentration (3%) of the ZnO nanorods with thickness $70 \pm 5 \mu\text{m}$ at different times of irradiation

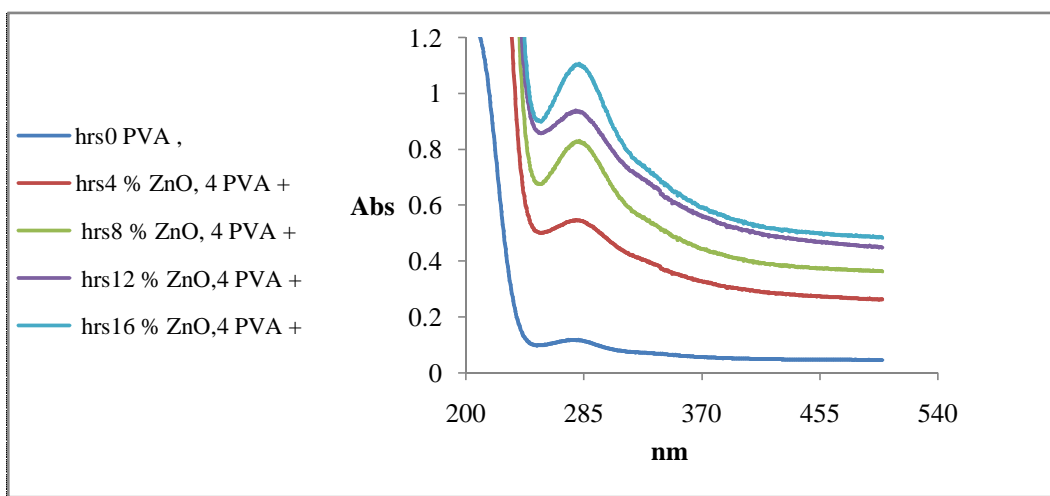


Fig. 10.Change in the spectrum of UV–Vis for PVAcontaining concentration (4%) of the ZnO nanorods with thickness $70 \pm 5 \mu\text{m}$ at different times of irradiation





Ahmed Mishaal Mohammed et al.

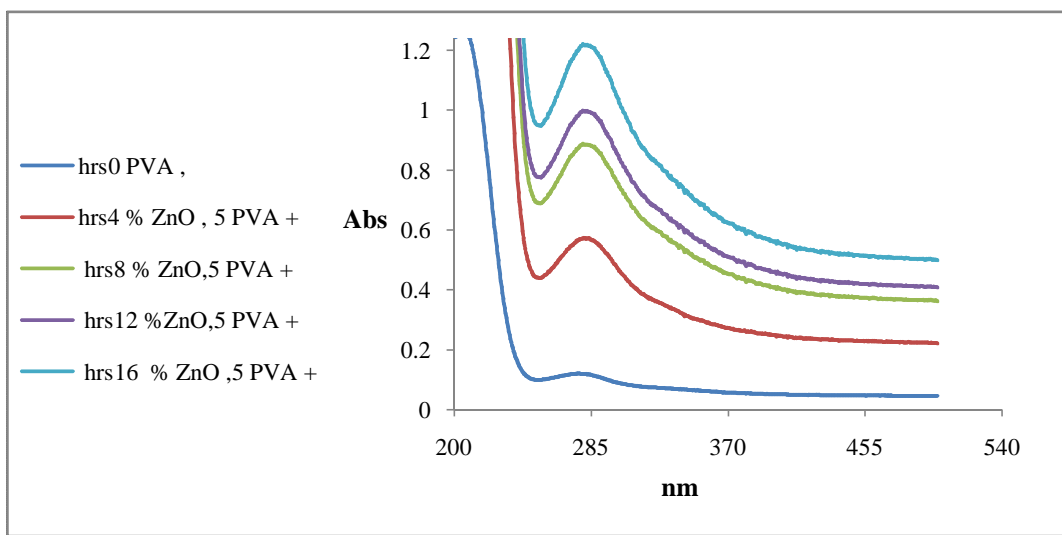


Fig. 11. Change in the spectrum of UV-Vis for PVA containing concentration (5%) of the ZnO nanorods with thickness $70 \pm 5 \mu\text{m}$ at different times of irradiation

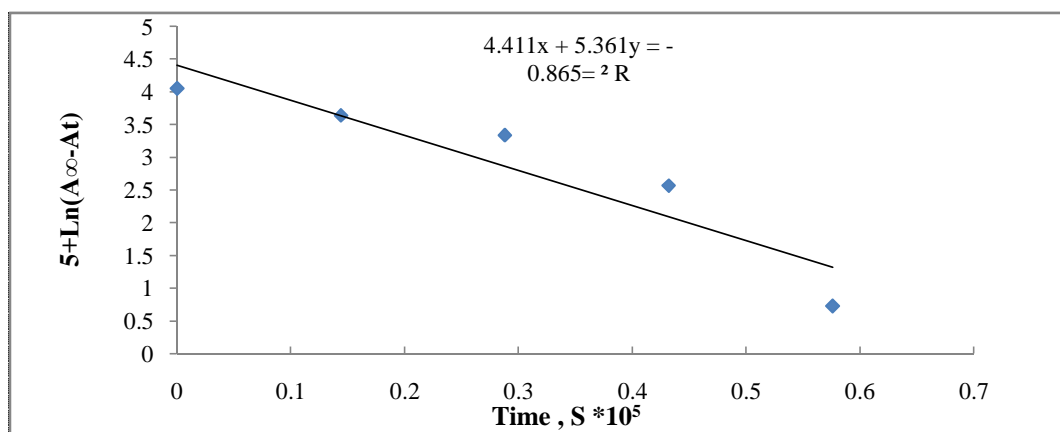


Fig. 12. The relationship between the logarithm of PVA films containing of ZnO nanorods with thickness $70 \pm 5 \mu\text{m}$ and concentration (1%) with irradiation time





Ahmed Mishaal Mohammed et al.

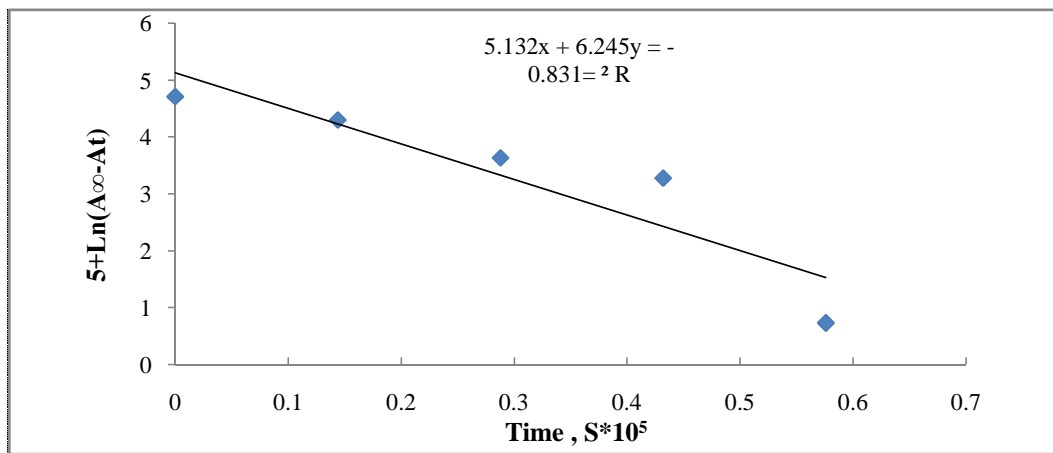


Fig. 13. The relationship between the logarithm of PVA films containing of ZnO nanorods with thickness $70 \pm 5 \mu\text{m}$ and concentration (2%) with irradiation time

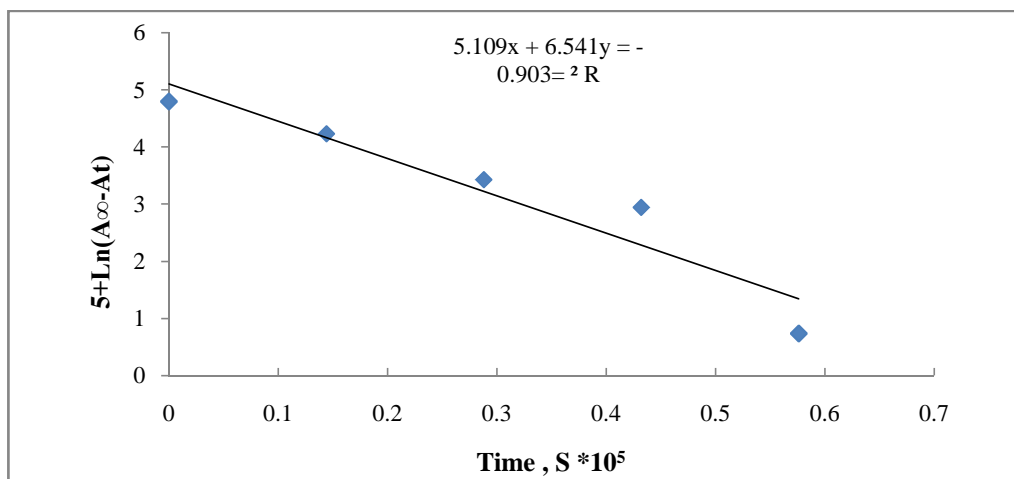


Fig. 14. The relationship between the logarithm of PVA films containing of ZnO nanorods with thickness $70 \pm 5 \mu\text{m}$ and concentration (3%) with irradiation time





Ahmed Mishaal Mohammed *et al.*

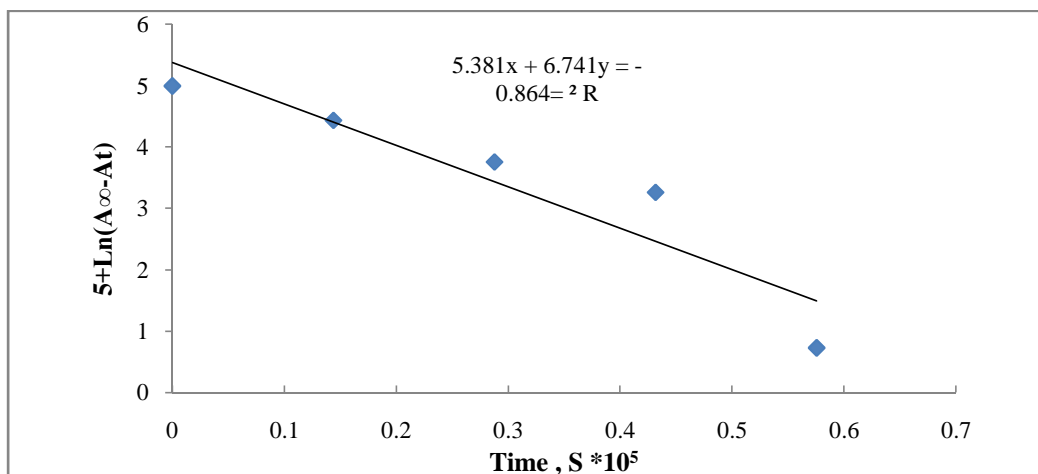


Fig. 15. The relationship between the logarithm of PVA films containing of ZnO nanorods with thickness $70 \pm 5 \mu\text{m}$ and concentration (4%) with irradiation time

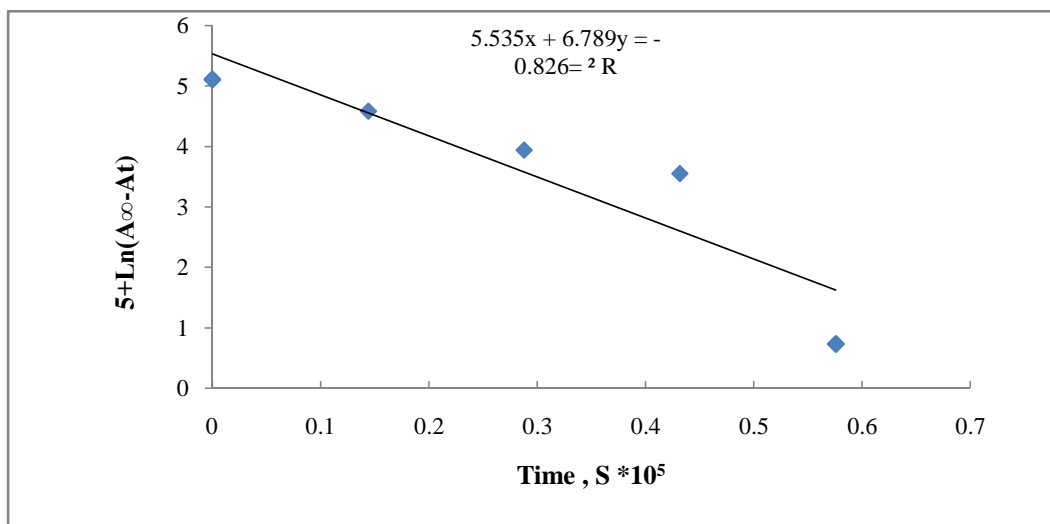


Fig. 16. The relationship between the logarithm of PVA films containing of ZnO nanorods with thickness $70 \pm 5 \mu\text{m}$ and concentration (5%) with irradiation time





Ahmed Mishaal Mohammed *et al.*

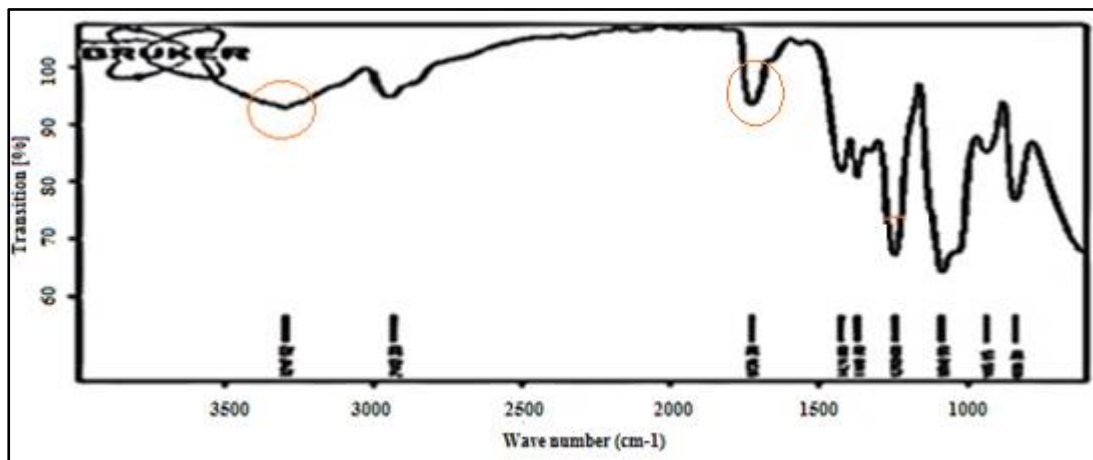


Fig. 17. FT-IR spectrum of pure PVA film with thickness $70\pm 5 \mu\text{m}$ before irradiation

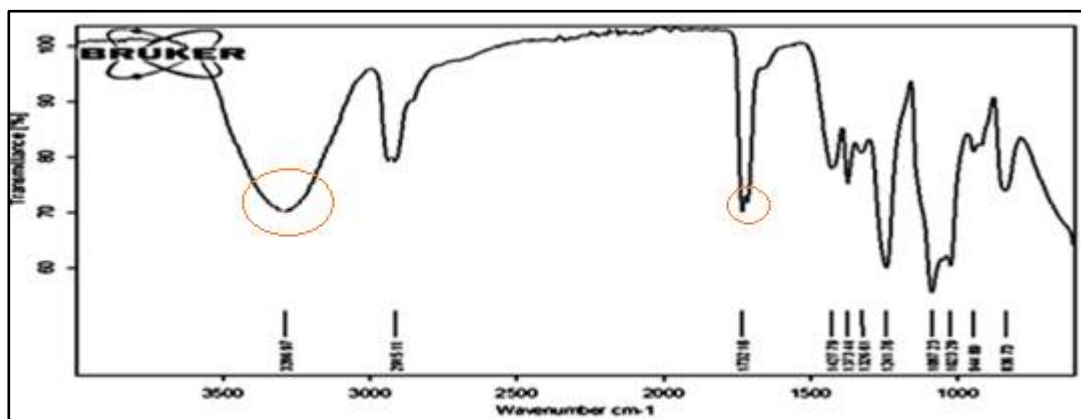


Fig. 18. FT-IR spectrum of pure PVA film with thickness $70\pm 5 \mu\text{m}$ and the time of irradiation 16 hrs.

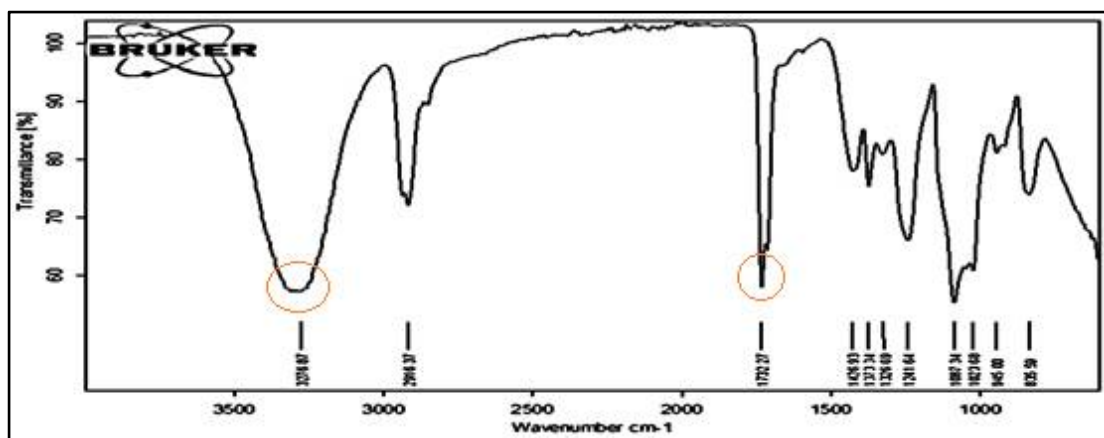


Fig. 19. FT-IR spectrum of PVA film with thickness $70\pm 5 \mu\text{m}$ containing concentration (5 %) of the ZnO nanorods and the time of irradiation 16 hrs.





Ahmed Mishaal Mohammed et al.

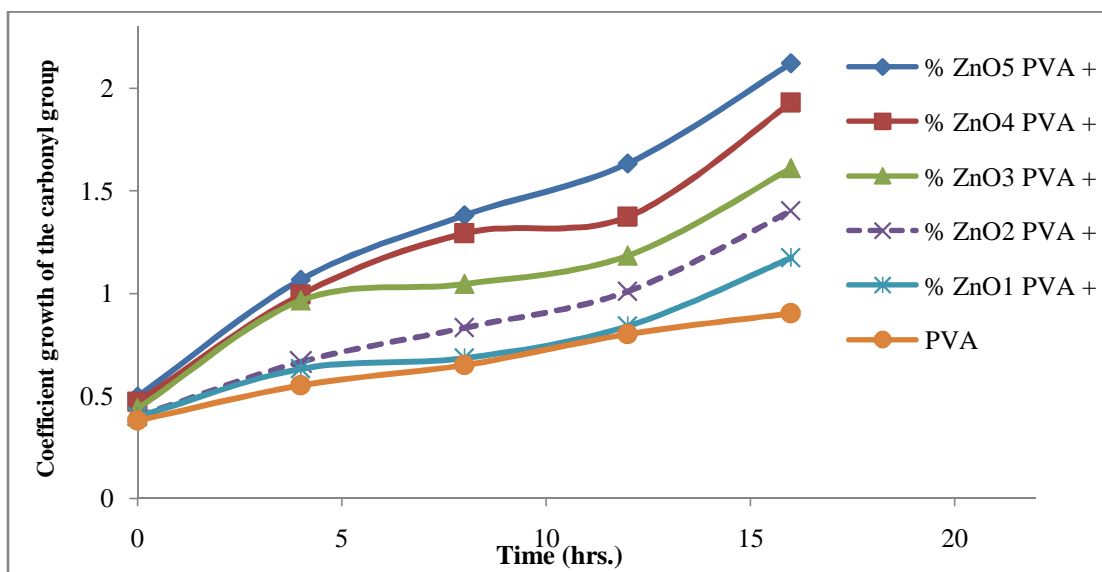


Fig. 20. The relationship between the absorption coefficient of the carbonyl and irradiation time of the results listed in the (Table 4)

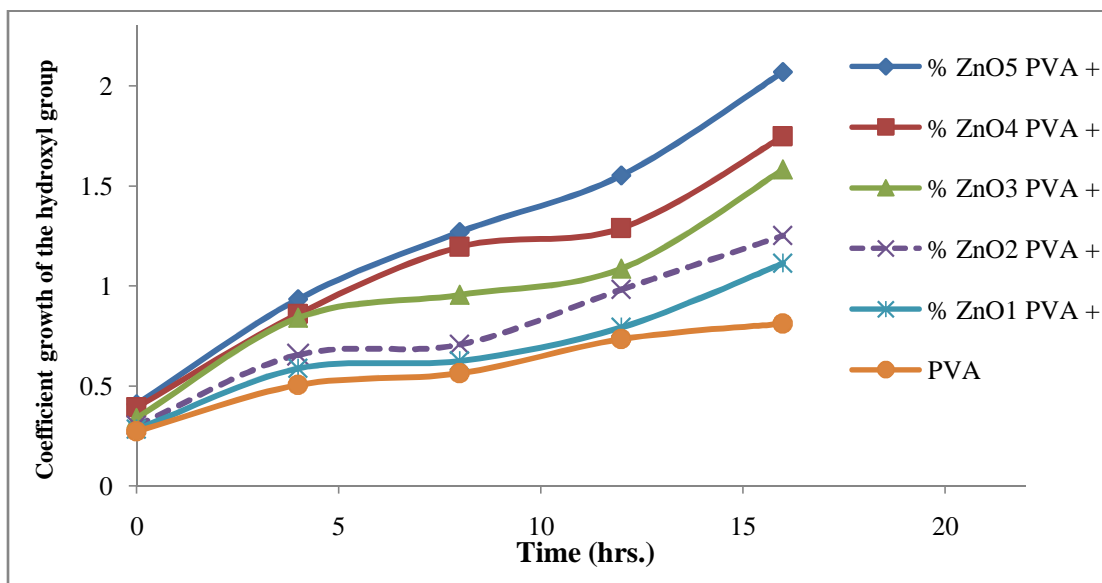


Fig. 21. The relationship between the absorption coefficient of the hydroxyl and irradiation time of the results listed in the (Table 5)

